Localized Effective Charges in Diatomic Crystals*

G. Lucovsky and Richard M. Martin
Xerox Palo Alto Research Center, Palo Alto, California 94304

and

E. Burstein†
Department of Physics, and Laboratory for Research on the Structure of Matter, University of Pennsylvania, Philadelphia, Pennsylvania 19104

(Received 30 April 1971)

We develop a model for simple diatomic crystals in which two effective-charge parameters are associated with the infrared-active optical-phonon mode. One of these is e_T^*, the macroscopic effective charge. The definition of the second charge, here designated as e_l^*, the localized effective charge, is model dependent and derived from a model which includes two contributions to the TO-phonon frequency. One of these is a mechanical or spring-constant contribution ω_0^2 and the second a frequency term which provides a measure of dipole-dipole interactions. e_l^* is computed from the experimental values of the TO-phonon frequencies and values of ω_0^2 calculated from simple force-constant models. For the zinc-blende (ZB) and wurtzite (W) crystals, $e_l^* \simeq f_i z_{eff}$, where f_i is the fractional ionicity and Z_{eff} is the effective chemical valence. For the rocksalt (NaCl) and CsCl crystals, e_l^* is not proportional to f_i, but instead shows systematic variations with ion size parameters. For the ten-electron NaCl and CsCl crystals, $e_T^* \propto \epsilon_\infty^{1/2}$, where ϵ_∞ is the optical-frequency dielectric constant. The model calculation for e_l^* is more reliable for the ZB and W crystals than the NaCl and CsCl crystals.

I. INTRODUCTION

The frequencies of the long-wavelength ($\vec{q} \simeq 0$) TO and LO phonons (ω_{TO}^2 and ω_{LO}^2) and the optical-frequency and static-dielectric constants (ϵ_∞ and ϵ_0), are known for a majority of the simple diatomic crystals, e.g., the covalently coordinated zinc-blende (ZB) and wurtzite (W) crystals[1] and the ionic NaCl- and CsCl-type crystals.[2] In these crystals, the oscillator strength of the TO phonon is reflected in the difference in the squares of the LO- and TO-phonon frequencies (or alternatively, via the Lyddane-Sachs-Teller relationship, in the difference between the optical-frequency and static-dielectric constants) and is commonly described by either of two effective-charge parameters e_T^* the macroscopic (transverse) effective charge,[3] or $e_s^*[= 3e_T^*/(\epsilon_\infty + 2)]$, the so-called Szigeti effective charge.[4] Of these two charges, the macroscopic effective charge is model independent and is calculated from readily observable quantities. On the other hand, the definition of any derived parameter describing charges at specific positions in the crystal, e.g., e_s^* is model dependent, in particular, requiring assumptions on the form of the effective field.

In this paper, an alternative approach is taken to the definition of a derived effective-charge parameter. We use a model in which two effective charges are associated with each TO-phonon mode. One of these is e_T^*, the macroscopic effective charge. e_T^* is a measure of the linear electric moment per unit cell and includes contributions from charge localized near the ion sites, as well as charge distributed throughout the unit cell.[2] On the other hand only localized charges give rise to dipolar forces which contribute to the TO-phonon frequency. We choose to assign the effective localized charges to be on the ion sites. The definition of the second charge is then based on a model which includes two contributions to the TO-phonon frequency. One of these is a "mechanical" or "spring-constant" frequency which is related through force-constant models to the elastic constants, and the other, an effective frequency derived from dipole-dipole interactions. The magnitude of the dipole interaction frequency yields the second effective-charge parameter e_l^* here designated as the localized effective charge. For the ZB and W crystals the local effective charge is shown to be proportional to the product of Z_{eff}, an effective chemical valence and f_i, the spectroscopic ionicity defined by Phillips and Van Vechten.[5] Similar results, but with more scatter, are found using the ionicity scale defined by Pauling.[6] On the other hand, in the NaCl- and CsCl-type crystals, the smaller variations in the calculated localized charge show no trend with ionicity.

The association of two or more effective charge parameters with each TO phonon is not a new concept. Burstein[7] suggested that there were two components to the macroscopic charge, such that

$$e_T^* = e_l^* + e_{nl}^* , \tag{1}$$

where e_{nl}^* is the nonlocalized charge. Making spe-

cific assumptions about the effective field, Burstein *et al.*[1] developed a relationship between ω_{TO}^2 and e_T^{*2}. The approach used in this paper is formally identical to the model of Ref. 1; however, here the charges are derived phenomenologically and no assumptions are made about their additivity. Verleur and Barker[8] and Ilegems and Pearson[9] have also used two charge models to describe the optical phonons in pseudobinary alloys of *W* and ZB crystals. In each case, values of e_l^* are obtained by assuming a nearest-neighbor central-force model for the mechanical frequency. The values of e_l^* so obtained are adjusted and used as parameters in fitting the reflectance spectra of the alloy crystals.

It should be noted that there are other ways of decomposing the macroscopic charge. The most prevalent is the division of e_T^* into rigid and dynamic[10] contributions; for example, in the polarizable ion[3] or shell models.[11] Here we make no attempt to distinguish rigid and dynamic contributions, both of which are inherently included in each of the charges discussed here.

One purpose of the present paper is to examine the variations in effective charges among the simple diatomic crystals. Trends in effective charges have been discussed previously,[12–14] in each case considering trends in the macroscopic charged e_T^* or a related quantity. Here we emphasize the trends in the localized charge e_l^*.

In Sec. II of the paper, we develop the analysis through which e_l^* can be calculated and then proceed to tabulate values for representative cubic crystals. In Sec. III, we examine the values of e_T^* and e_l^* for trends with other parameters, e.g., the spectroscopic ionicity, the ion sizes and the optical-frequency dielectric constant. In Sec. IV, we discuss our results.

II. MODELS OF INTERATOMIC FORCES

Our scheme is based on two equations which relate the phonon frequencies to "mechanical," plasma, and dipolar interaction frequencies:

$$\omega_{TO}^2 = \omega_0^2 - \Omega_{DD}^2 , \tag{2a}$$

$$\omega_{LO}^2 = \omega_{TO}^2 + \Omega_P^2 . \tag{2b}$$

Here ω_0^2 is the mechanical or spring-constant frequency which is related to the mechanical force constants with Coulomb forces subtracted, Ω_{DD} is an effective frequency characterizing dipole-dipole interactions, and Ω_P is a macroscopic plasma frequency describing the restoring force contribution of the macroscopic field to the LO phonon. The macroscopic plasma frequency is model independent and is given directly by (2b). In terms of the dimensionless macroscopic effective charge, e_T^*, one finds for diatomic cubic crystals[7]

$$\Omega_P^2 = \omega_{LO}^2 - \omega_{TO}^2 = (4\pi Ne^2/\bar{M})\, e_T^{*2}/\epsilon_\infty . \tag{3}$$

Here N is the ion pair density, $\bar{M}$ the reduced mass of the pair, and e the electron charge. The factor of $1/\epsilon_\infty$ incorporates rigorously the screening of the macroscopic field by the interband electronic transitions.

The decomposition of the restoring force for the TO phonon in (2a), on the other hand, is not unique,[3] since ω_0^2 and Ω_{DD}^2 are not directly observable. We choose to define Ω_{DD}^2 as the contribution to ω_{TO}^2 from point dipoles at the ion sites interacting in a vacuum. In terms of a localized effective charge e_l^*, which is essentially the localized moment generated per unit displacement of an ion, we find

$$\Omega_{DD}^2 = (4\pi Ne^2/3\bar{M})\, e_l^{*2} , \tag{4}$$

where the factor of $\frac{1}{3}$ reflects the cubic symmetry. All local field effects are implicitly included in e_l^*. The remaining contribution ω_0^2 arises from short range forces. The applicability of our procedure hinges upon the existence of a realistic model from which to evaluate such nondipolar forces.

We want to interpret e_l^* in Eq. (4) as a meaningful measure of the moment induced in the neighborhood of a given atom by the local atomic displacements.[4] This is valid if the renormalization of e_l^* due to local field effects can be neglected. Only if such an interpretation of e_l^* is tenable would one expect a direct correlation between e_l^* and a microscopic characterization such as the ionicity.

To make the argument more quantitative, let us assume that analogous to (1), the electron response in ϵ_∞ can be divided into local and nonlocal parts

$$\epsilon_\infty = 1 + 4\pi\chi_l + 4\pi\chi_{nl} . \tag{5}$$

In the spirit of Ref. 7, χ_l is assumed to be a localized susceptibility which describes the electron response to the short-wavelength "local" electric fields such as those accompanying a TO phonon, whereas the part of the susceptibility of χ_{nl} applies only to macroscopic electric fields which are absent for a TO phonon. In this approximation, in terms of a localized charged e_l^*, we would find

$$\Omega_{DD}^2 = (4\pi Ne^2/3M)\, e_l^{*2}\,[\tfrac{1}{3}(1 + 4\pi\chi_l + 2)] . \tag{6}$$

The final term is the Lorentz local field factor for cubic crystals. For ZnS structure crystals, Brodsky and Burstein[15] have argued that $\chi_l \ll \chi_{nl}$. Since we cannot determine χ_l directly, the most reasonable approximation is to set $\chi_l \to 0$ in which case Eq. (6) reduces to (4). For the alkali halides, we expect χ_l to be at most comparable to χ_{nl}. This argument is based on a Kramers-Kronig analysis of the contributions to the real and imaginary parts of the complex dielectric constant[16,17] where the demarcation point between localized and delocalized excitations is taken by us to be the threshold photon

TABLE I. Effective charges of the simple diatomic crystals. e_T^* is the macroscopic transverse effective charge and e_l^* the localized effective charge derived in the present work [Eqs. (2a) and (4)] within three different force-constant models: (i) CNN, (ii) Lundqvist model (Ref. 21) for NaCl and CsCl structure crystals, and (iii) KM model for zinc-blende and wurtzite structure crystals. Experimental quantities used for the following table are taken from Refs. 1, 2, 13, and 19.

Crystal	f_i	Z_{eff}	ϵ_∞	e_T^*	e_l^* CNN	e_l^* Lundqvist
			NaCl structure crystals			
			alkali halides •			
LiF	0.91	1.0	1.93	0.85	0.92	1.11
LiCl	0.90	1.0	2.75	1.23	1.12	1.15
LiBr	0.90	1.0	3.17	1.28	1.18	1.19
NaF	0.95	1.0	1.74	1.03	0.90	0.99
NaCl	0.94	1.0	2.33	1.11	0.94	0.95
NaBr	0.93	1.0	2.60	1.13	0.94	0.94
NaI	0.93	1.0	3.01	1.25	1.01	0.89
KF	0.96	1.0	1.85	1.17	0.96	0.90
KCl	0.95	1.0	2.17	1.13	0.86	0.87
KBr	0.95	1.0	2.36	1.13	0.94	0.87
KI	0.95	1.0	2.65	1.17	0.80	0.78
RbF	0.96	1.0	1.93	1.28	1.04	0.96
RbCl	0.96	1.0	2.18	1.16	0.94	0.87
RbBr	0.96	1.0	2.34	1.15	0.91	0.82
RbI	0.95	1.0	2.58	1.17	0.87	0.75
			alkaline oxides			
MgO	0.84	2.0	2.95	1.77	1.49	1.92
CaO	0.91	2.0	3.33	1.96	1.74	1.96
SrO	0.93	2.0	3.46	2.11	1.83	1.98
			eight-electron, non-rare-gas configuration crystals			
AgCl	0.86	1.5	3.92	1.37	1.54	0.47
AgBr	0.86	1.5	4.62	1.50	1.58	0.57
CdO	0.79	2.0	5.40	2.91	...	...
			ten-electron, non-rare-gas configuration crystals			
PbS	≃0.75	3.0	17.2	4.8	2.40	2.28
PbSe	≃0.80	3.0	22.9	5.8	2.31	...
PbTe	≃0.70	3.0	32.8	6.5	2.29	2.45
SnTe	≃0.70	3.0	45.0	8.1	2.16	2.33
			CsCl structure crystals			
			rare-gas configuration ions			
CsCl	≃0.98	1.0	2.63	1.31	1.00	0.90
CsBr	≃0.98	1.0	2.78	1.30	0.91	0.84
CsI	≃0.98	1.0	3.02	1.31	0.91	0.87
			ten-electron non-rare-gas configuration			
TlCl	≃0.90	2.0	4.76	1.96	1.30	1.00
TlBr	≃0.90	2.0	5.34	2.06	1.34	1.03
			Zinc-blende			
CuCl	0.75	1.5	3.6	1.12	1.50	1.51
CuBr	0.74	1.5	4.4	1.49	1.32	1.38
CuI	0.69	1.5	5.2	2.40	1.69	1.74
AgI	0.77	1.5	4.9	1.40	1.38	1.38
ZnS	0.62	2.0	5.1	2.15	1.75	1.84
ZnSe	0.63	2.0	5.9	2.03	1.56	1.69
ZnTe	0.61	2.0	7.3	2.00	1.58	1.74
CdTe	0.72	2.0	7.3	2.35	1.67	1.76
HgTe	≃0.75	2.0	14.0	2.96	2.02	2.03

TABLE I (*Continued*).

Crystal	f_i	Z_{eff}	ϵ_∞	e_T^*	e_l^* CNN	e_l^* Lundqvist
			Zinc-blende			
BN	0.26	3.0	4.5	2.47	...	...
AlP	0.31	3.0	7.6	2.28	...	...
AlAs	0.27	3.0	9.0	2.30	...	...
AlSb	0.43	3.0	10.2	1.93	0.81	1.28
GaP	0.33	3.0	8.5	2.04	0.96	1.41
GaAs	0.31	3.0	10.9	2.16	0.78	1.28
GaSb	0.26	3.0	14.4	2.15	0.41	0.97
InP	0.42	3.0	9.6	2.55	1.36	1.61
InAs	0.36	3.0	12.3	2.53	1.01	1.16
InSb	0.32	3.0	15.6	2.42	0.53	0.91
SiC	0.18	4.0	6.7	2.57	0.60	0.95
			Wurtzite			
BeO	0.60	2.0	3.0	1.83	1.76	1.94
ZnO	0.62	2.0	3.7	2.09	1.91	2.05
CdS	0.69	2.0	5.6	2.27	1.79	1.93
CdSe	0.70	2.0	6.2	2.25	1.73	1.85
GaN	0.50	3.0	5.8	3.20	...	...
AlN	0.45	3.0	4.7	2.75	...	...

energy for strong photoconductive effects.[17] For a unified treatment of ZnS, NaCl, and CsCl structure crystals, we derive e_l^* from Eq. (4). Corrections to e_l^* due to screening and local field effects are expected to be $< 15\%$ for the entire series of crystals.

The most serious problem is evaluating ω_0^2 sufficiently accurately to calculate Ω_{DD}^2 from (2a). The only additional pieces of information available for the calculation of ω_0^2 for the entire range of crystals are the elastic constants C_{ij}. Therefore, we require simple, yet realistic, force-constant models with parameters adjusted to fit selected C_{ij}. It is convenient at this point to introduce the dimensionless or reduced constants defined by Keyes[18]

$$C_{ij}^* = C_{ij}/C_0 , \quad C_0 = e^2/r_0^4 , \tag{7}$$

where r_0 is the nearest-neighbor distance.

If one assumes that there are only central nearest-neighbor (CNN) short-range forces acting on the effective ion cores, then it may be shown that[3,4]

$$\omega_0^2 = (3v_a e^2/r_0^6 \bar{M})\, B^* , \tag{8}$$

where v_a is the volume per ion pair and B^* is the reduced bulk modulus $[= \frac{1}{3}(C_{11}^* + 2C_{12}^*)$ for cubic crystals]. In Table I, we have included values of e_l^* calculated from Eqs. (2a), (4), and (8) and the experimental B^* [13,19] and ω_{TO}.[1,2] One ramification of such a central-force model for centrosymmetric crystals, such as NaCl and CsCl, is a relation among the elastic constants,[20] namely, the Cauchy relation $C_{12} = C_{44}$. This does not hold for real crystals and Lundqvist[21] has developed a simple model for NaCl crystals, in which noncentral three-body forces account for the failure of the Cauchy relation. In the Lundqvist formulation for NaCl crystals one finds

$$\omega_0^2 = 12(Ne^2/\bar{M})\,(B^* + C_{44}^* - C_{12}^*) , \tag{9}$$

so that the difference in the square of the mechanical frequency as calculated in the Lundqvist and the central-force models is simply related to the failure of the Cauchy relation. Included in Table I are values of e_l^* for the NaCl crystals as calculated using this model. We have also calculated e_l^* for the CsCl crystals, assuming that the first-order correction to the corresponding expression for ω_0^2 is also given by Eq. (9).

For ZB crystals, Keating[22] and Martin[13] (KM) have shown that noncentral forces are important. Including a bond-bending noncentral force as done by KM, one finds

$$\omega_0^2 = (\tfrac{16}{3})^2 (Ne^2/\bar{M})\,(B^* + \tfrac{1}{6}\beta^*) , \tag{10}$$

where β^* is a reduced bond-bending force constant.[13] In order to derive β^* from measured elastic constants, a model for Coulomb contributions to the elastic constants is necessary. We use Martin's results[13] but require that dipole interaction contributions to the C_{ij}'s be described by e_l^{*2} instead of the S parameter used by Martin[13]; this leads to

$$\beta^* = C_{11}^* - C_{12}^* - 0.052\, e_l^{*2} . \tag{11}$$

Equations (2a), (4), (10), and (11) are sufficient to

TABLE II. Fractional difference $\Delta = (\omega_0^2 - \omega_{TO}^2)/\omega_{TO}^2$ between observed TO-phonon frequency ω_{TO} and that predicted by the CNN and KM models for homopolar crystals.

Crystal	CNN	KM
Si	−0.10	0.09
Ge	−0.16	0.04

determine e_I^* for ZB crystals, the values of which are listed in the final column of Table I.

In Table I, we have included e_T^* and e_I^* values for wurtzite crystals. These are average values derived from $\bar{\omega}_{LO}^2 = \frac{1}{3}[\omega_{LO}^2(A_1) + 2\omega_{LO}^2(E_1)]$ and a similar expression for $\bar{\omega}_{TO}^2$. To calculate ω_0^2, we have used Eq. (10) with the small contribution from β^* interpolated from the values of β^* in ZB crystals of similar ionicity.

The reliability of the localized charges e_I^* given in Table I depends upon the accuracy of ω_0^2 computed from the models. One way to test the model for ZB crystals is to apply it to Si or Ge where $e_T^* = e_I^* = 0$. We can define

$$\Delta \equiv (\omega_0^2 - \omega_{TO}^2)/\omega_{TO}^2 \tag{12}$$

as a measure of the accuracy of our procedure. The values of Δ are listed in Table II where we see that ω_0^2 is too large in the KM model and too small in the central-force model. Therefore, we expect that the true values of e_I^* for the diatomic ZB and W crystals are bracketed by the results of the two-model calculations.

III. TRENDS IN EFFECTIVE-CHARGE PARAMETERS

Part of the motivation for this paper originated from attempts to find systematic trends in the effective-charge parameters with variables such as the spectroscopic ionicity or the optical-frequency dielectric constant. We now show how our procedure for calculating e_I^* leads to the identification of trends in that parameter, with ionicity for the ZB and W crystals but with the nearest-neighbor distance for the NaCl crystals.

A. ZB and W Crystals

In order to discuss trends in effective charge parameters with ionicity, we first set the framework for the discussion by giving the most naive relationship between ionicity and an effective charge parameter. Consider a crystal $A^{8-Z}B^Z$, where Z is the classical chemical valence. If the crystal were composed of point-charge ions residing on the lattice sites, and if these charges were the only ones that contributed to the effective Coulomb forces, then we would expect

$$e_T^* = e_I^* \simeq Zf_i \ . \tag{13}$$

Since there are both localized and nonlocalized, as well as static and dynamic contributions to both e_T^* and e_I^*, we expect the situation in real crystals to differ from Eq. (13). For example, as shown in Table I, $e_T^* \neq e_I^*$ for all of the crystals studied. Further, the work of Van Vechten[5] and others[12] indicates that there are crystals wherein Z may differ from the classical chemical valence. In interpreting the value of C, the heteropolar energy gap, for the Ag and Cu halides, Van Vechten[5] used a value of $Z = 2$ for the Ag and Cu ions and a value of $Z = 1$ for the halide ions. We follow a similar procedure, defining an effective classical valence Z_{eff} by

$$Z_{eff} = \tfrac{1}{2}(Z_A + Z_B) \ , \tag{14}$$

where Z_A and Z_B are the principal valence states of the elements composing the crystal, e.g., $Z_A = 2$ for Cu, Ag; $Z_A = 3$ for Tl; and $Z_A = 4$ for Pb, Sn.

In Fig. 1, we show a plot of e_T^*/Z_{eff} vs f_i for the ZB and W crystals. With the exception of the I-VII ZB crystals (CuCl, CuBr, CuI, and AgI), e_T^*/Z_{eff} increases approximately linearly with f_i; however, the plot does not extrapolate to zero as $f_i \to 0$, as it should for the homopolar semiconductors C, Si, Ge, and α-Sn. On the other hand, as shown in Fig. 2 a plot of e_I^*/Z_{eff} shows a strong trend with ionicity and a line can be drawn that extrapolates to zero for $f_i \to 0$. Note that the scatter for the II-VI and I-VII crystals ($f_i \simeq 0.6 - 0.77$) is greater than that of the other crystals (SiC and the III-V, ZB crystals). This is related, in part, to the greater uncertainty in the data for the II-VI's and

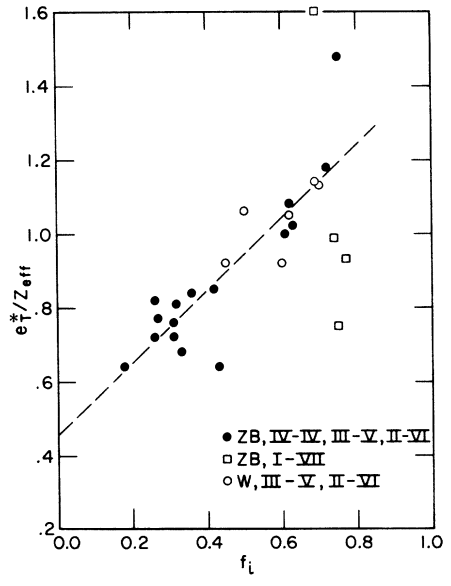

FIG. 1. Normalized macroscopic transverse charge e_T^*/Z_{eff} for zinc-blende and wurtzite crystals vs the ionicity f_i.

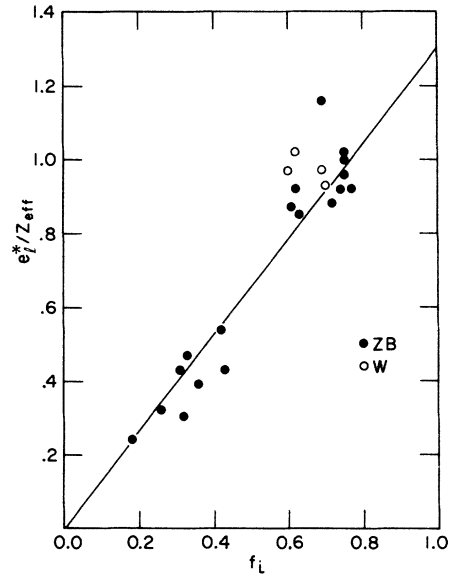

FIG. 2. Normalized localized effective charge e_i^*/Z_{eff} for zinc-blende and wurtzite crystals in KM model vs the ionicity f_i. Note that in contrast to e_T^*/Z_{eff} are well described by a line that passes through 0 at $f_i = 0$.

I-VII's compared to the III-V's, and also to the KM model becoming less accurate for the more ionic crystals. The e_i^* values in Fig. 2 are those obtained using the KM model for ω_0^2. The values of e_i^* obtained using the CNN model for ω_0^2 also show a trend with ionicity; however, there is somewhat greater scatter in the values of e_i^*/Z_{eff} using CNN model for ω_0^2. The slope of the e_i^*/Z_{eff} vs f_i plot is 1.3.

There are two other linear trends in effective-charge parameters with ionicity that hold for SiC and the III-V and II-VI crystals but not for the ZB I-VII crystals. These are

$$(e_i^*/e_T^*)^2 \simeq f_i \tag{15}$$

and

$$e_T^{*2}/\epsilon_\infty \simeq f_i \ . \tag{16}$$

The latter trend was noted previously in Ref. 13. The I-VII crystals have anomalously low values of e_T^*, so that $(e_i^*/e_T^*)^2$ and e_T^{*2}/ϵ_∞ are, respectively, high and low compared to the trend followed by the other crystals.

B. NaCl and CsCl Crystals

In the tetrahedrally coordinated ZB and *W* crystals, the ionicity scale of Phillips and Van Vechten[5] was found to be a useful scale for understanding trends in e_T^*/Z_{eff} and e_i^*/Z_{eff}. The more ionic NaCl- and CsCl-type crystals also support the same general trend as may be seen from Table I. However, within the range of these crystals, there is much more scatter, and it is clear that variables other than the ionicity are necessary to describe any trends. The role of ionic sizes[6] in determining many of the properties of the NaCl and CsCl crystals has been emphasized in the literature. We find that within the framework of the Lundqvist model[21] for ω_0^2 the interatomic separation r_0 does provide an appropriate scale for discussing trends in e_i^*.

In this model calculation e_i^* is a linear function of r_0 for each family of alkali halide crystals. However, e_i^* vs r_0, as calculated using the CNN model for ω_0^2, shows considerably greater scatter to the extent that the trends with r_0 are not clearly defined. This is to be contrasted with the model calculations for the ZB and *W* crystals, where plots of e_i^*/Z_{eff} vs f_i show the same trends with ionicity when ω_0^2 is calculated from the CNN model or the KM model. In the Lundqvist model,[21] for the Li salts e_i^* increases with increasing r_0, whereas in the Na, K, and Rb salts e_i^* decreases with increasing r_0. The fact that Li salts appear to behave differently from the others may be a figment of the model rather than a real effect. Next-nearest-neighbor halide-halide interactions[5,23] are more important in the Li salts because of the small Li^+ size. Taking such forces into account would tend to lower the calculated values of e_i^* from those given in Table I, with larger decreases for larger radius anions. This effect is not expected to be as important as the other salts, and in any case should still yield a smooth downward trend in e_i^* with radius, within each family of crystals.

Another group of compounds, crystallizing in the NaCl or CsCl structures, are the crystals which nominally have ten valence electrons, i.e., PbS, PbSe, PbTe, SnTe, TlCl, and TlBr. The "extra" electrons apparently increase both e_T^* and the dielectric constant ϵ_∞ in comparison to the "normal" eight-electron crystals.[24] To test the hypothesis that the two effects are related, e_T^* and e_T^*/Z_{eff} vs ϵ_∞ are plotted in Fig. 3. We see that over a wide range $e_T^*/Z_{eff} \propto \epsilon_\infty^{1/2}$. Thus in these crystals e_T^*, ϵ_∞, ω_{TO} and other properties vary widely but the normalized splitting of the LO and TO frequencies squared, $4\pi e_T^{*2}/\epsilon_\infty$, remains roughly constant. This is in marked contrast to the eight-electron crystals and is particularly important in understanding the tendency toward ferroelectricity in these compounds.

IV. DISCUSSION

We have shown that the localized effective charge e_i^* scales linearly with the classical valence multiplied by the spectroscopic ionicity for a wide range of ionicity (0 to 0.75) for tetrahedrally coordinated crystals. This is appealing in that it states that the charge displaced in the vicinity of an atom by the motion of that atom and its near neighbors is proportional to the crystal ionicity. The non-

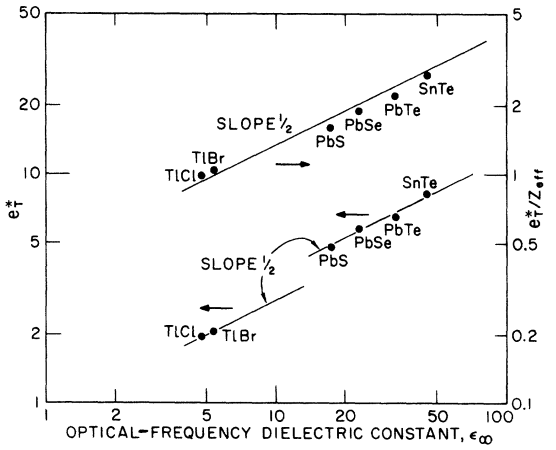

FIG. 3. Transverse macroscopic charge e_T^*/Z_{eff} vs ϵ_∞ for the "non-rare-gas" configuration ten-electron NaCl and CsCl structure crystals. The data suggest $e_T^* \propto \epsilon_\infty^{1/2}$ or $(e_T^*/Z_{eff})^2/\epsilon_\infty \simeq$ const.

local displaced charge, which is incorporated in e_T^*, on the other hand, is not so simply related to the ionic character so that e_T^* is more complicated. This is especially evident in the I-VII tetrahedrally coordinated crystals where $e_t^*/Z_{eff} \simeq f_i$, but e_T^*/Z_{eff} differs greatly from the II-VI materials of similar ionicity.

The NaCl and CsCl crystals on the other hand span only a small ionicity range but show a large amount of scatter in e_t^*. The other dominant factor which must be taken into account to explain the trends in e_t^* in these ionic crystals are the relative ion sizes. The model we have used is not as satisfactory for the NaCl or CsCl crystals, as for ZB or *W* crystals, because possible errors due to neglect of local field effects and second-neighbor anion-anion interaction (double repulsion) may be as large as the differences in e_t^* over the entire range of crystals. Nevertheless, because the above corrections should also be simple functions of ion sizes, the conclusion remains that ionicity as defined by Pauling[6] or by Phillips and Van Vechten,[5] is not the dominant factor in determining the variations in the effective charges in the ionic crystals.

Lawaetz has presented a correlation of e_s^*/Z_{eff} with $C/\hbar\omega_p$ where $\hbar\omega$ is the valence electron plasma frequency and *C* the heteropolar energy gap. He finds that $C/\hbar\omega_p$ is a much better parameter than f_i in the NaCl crystals. Further, for the ZB and *W* crystals, unlike e_T^*/Z_{eff}, e_s^*/Z_{eff} tends toward zero as *C* or $f_i \to 0$. Arguments indicate that the full local field factor $\frac{1}{3}(\epsilon_\infty + 2)$, used to derive e_s^* is not tenable, especially in the more covalent crystals,[15] so that $e_s^* \to 0$ as $f_i \to 0$ may be fortuitous.

Burstein *et al.*[1] observed that the reduced-LO-phonon frequencies, $\omega_{LO}^* \equiv \omega_{LO}\,(e^2/\bar{M}r_0^3)^{1/2}$ of the III-V and II-VI crystals were essentially constant for each group of crystals. They conjectured that since there were two effective-charge contributions of opposite sign to ω_{LO}^{*2}, that these cancelled and that the consistency in ω_{LO}^{*2} reflected a consistency in ω_0^{*2}. This is indeed the case, specifically

$$\omega_{LO}^2 = \omega_0^2 + (4\pi Ne^2/\bar{M})\,[e_T^{*2}/\epsilon_\infty - \tfrac{1}{3}e_t^{*2}] \tag{17}$$

or in terms of reduced frequencies and using the KM model for ω_0^2, we have

$$\omega_{LO}^{*2} \propto k_1\{B^* + \tfrac{1}{6}\beta^*\} + (e_T^{*2}/\epsilon_\infty - \tfrac{1}{3}e_t^{*2})\,, \tag{18}$$

where k_1 is a constant. For both the III-V and II-VI crystals, the second term in parenthesis is small and the first term in curly brackets is approximately a constant. Therefore, to within a factor of better than 10%, the Burstein *et al.* result is accounted for quantitatively.

We have used the spectroscopic scale defined by Phillips and Van Vechten[5] as our measure of ionicity. It should be noted that for the most part, very similar results would be found using Pauling's scale.[6] The primary difference in using Pauling's scale is a grouping of the III-V compounds near 0.26 ionicity and a spreading out of the alkali halides with much scatter remaining.

V. SUMMARY

We have developed a procedure for calculating a local effective-charge parameter for the lattice modes in diatomic crystals. The procedure is based on decomposition of the TO-phonon frequency into two components, one associated with short-range forces and one with dipolar interactions. By applying the calculation of the nondipolar component to Si and Ge, we find that the model calculation of ω_0^2 is sufficiently accurate for the ZB and *W* crystals. On the other hand, the models used for the decomposition of ω_{TO}^2 for the NaCl and CsCl crystals are somewhat more speculative. The localized charge is found to scale with classical valence and ionicity for ZB and *W* crystals, but depends more strongly on other parameters, e.g., relative ion size, in NaCl or CsCl crystals.

---

*A preliminary version of this paper was presented at the March, 1971 APS Meeting [Bull. Am. Phys. Soc. 16, 427 (1971)].

†Research supported in part by U. S. Office of Naval Research.

[1] E. Burstein, A. Pinczuk, and R. F. Wallis, in *Proceedings of the Conference on the Physics of Semimetals and Narrow Gap Semiconductors*, edited by D. L. Carter and R. T. Bate (Pergamon, N. Y., 1971), p. 251.

[2] E. Burstein, M. H. Brodsky, and G. Lucovsky, Int.

J. Quantum Chem. 15, 759 (1967).
[3]M. Born and K. Huang, *Dynamical Theory of Crystal Lattices* (Clarendon, Oxford, England, 1954), Chap. 2.
[4]B. Szigeti, Trans. Faraday Soc. 45, 155 (1949).
[5]J. C. Phillips, Rev. Mod. Phys. 42, 317 (1970); J. A. Van Vechten, Phys. Rev. 182, 891 (1969).
[6]L. Pauling, *The Nature of the Chemical Bond*, 2nd ed. (Cornell U. P., Ithaca, N. Y., 1939).
[7]E. Burstein, J. Phys. Chem. Solids Suppl. 21, 315 (1965).
[8]H. W. Verleur and A. S. Barker, Jr., Phys. Rev. 149, 715 (1966); 155, 750 (1967).
[9]M. Ilegems and G. L. Pearson, Phys. Rev. B 1, 1576 (1970).
[10]W. Cochran, Nature 191, 60 (1961).
[11]B. G. Dick and A. Overhauser, Phys. Rev. 112, 90 (1958).
[12]P. Lawaetz. Phys. Rev. Letters 26, 697 (1971).
[13]R. M. Martin, Phys. Rev. B 1, 4005 (1970).
[14]J. Tateno, J. Phys. Chem. Solids 31, 1641 (1970).
[15]M. H. Brodsky and E. Burstein, Bull. Am. Phys. Soc. 7, 214 (1962).
[16]H. R. Philipp and H. Ehrenreich, Phys. Rev. 131, 2016 (1963).
[17]J. E. Eby, K. J. Teegarden, and D. B. Dutton, Phys. Rev. 116, 1099 (1959); E. A. Taft and H. R. Philipp, J. Phys. Chem. Solids 3, 1 (1959); J. W. Taylor and P. L. Hartman, Phys. Rev. 113, 1421 (1959).
[18]R. W. Keyes, J. Appl. Phys. 33, 3371 (1962).
[19]H. B. Huntington, in *Solid State Physics*, edited by F. Seitz and D. Turnbull (Academic, New York, 1958), Vol. 7; and in *Landolt–Bornstein Numerical Data and Functional Relationships in Science and Technology, New Series*, edited by K. H. Hellewege (Springer, Berlin, 1966), Group 3, Band 5.
[20]M. Born and K. Huang, *Dynamical Theory of Crystal Lattices* (Clarendon, Oxford, England, 1954), Chap. 3.
[21]S. O. Lundqvist, Arkiv Fysik 9, 435 (1955).
[22]P. N. Keating, Phys. Rev. 145, 637 (1966).
[23]J. Vallin, G. Pettersson, J. L. Calais, and K. Mansikka, Arkiv Fysik 34, 199 (1967).
[24]E. Burstein and G. Lucovsky, Bull. Am. Phys. Soc. 16, 427 (1971).

PHYSICAL REVIEW B VOLUME 4, NUMBER 4 15 AUGUST 1971

Electronic Structure of NaBr†

A. Barry Kunz and Nunzio O. Lipari
Department of Physics and Materials Research Laboratory, University of Illinois, Urbana, Illinois 61801
(Received 19 February 1971)

In this paper, *ab initio* energy bands for NaBr are obtained by means of the nonrelativistic mixed-basis (MB) method. The calculation is performed self-consistently in the Hartree-Fock limit, accurate to first order in interatomic overlap. We assume the core states to be nonoverlapping. Koopman's theorem is assumed here. Correlation effects are then included and are found to be important in that they reduce substantially the band gap, and also the widths of the valence bands. The resultant bands are fitted with a pseudopotential and the density of states of the valence and conduction bands are obtained as are the joint density of states for both valence and core excitations. These results are compared to recent optical and soft-x-ray absorption studies of NaBr, and the valence results are compared to x-ray emission studies. The experimental comparisons favor the more distinctive results of this calculation such as the wide (4 eV)4*p* valence bands and the structured state density of the conduction bands.

I. INTRODUCTION

Despite the great deal of effort expended in recent years on calculating the energy bands of insulating crystals, agreement between the results of different calculations for the same material is generally not obtained.[1] This discrepancy between the different calculations is due in part to the differing assumptions made in forming the crystal potential.[2] Therefore, it seems useful to obtain energy bands *ab initio* whenever possible. This means that for insulating solids, one should use the correct Fock operator, self-consistently if possible, and should correct for correlation effects.[3] There were some early attempts to produce such *ab initio* calculations[4] but these were by tight-binding techniques and limited to the valence and the lowest conduction band.

Recently the authors, individually and jointly, have made considerable progress in obtaining *ab initio* energy bands for these materials.[5] It has been seen from these calculations for LiCl, LiBr, NaCl, Ar, and Kr that the *ab initio* energy bands differ substantially from those obtained using approximate exchange potentials.

One of us (A. B. K.) has developed a local-orbitals theory[6] which allows us to obtain accurate self-consistent charge densities for alkali halide crystals in their ground state in the Hartree-Fock limit. These orbitals are accurate to first order